Applied Microbiology and Biotechnology (2018) 102:2379–2389
https://doi.org/10.1007/s00253-018-8768-0

ENVIRONMENTAL BIOTECHNOLOGY

Single-stage autotrophic nitrogen removal process at high loading rate: granular reactor performance, kinetics, and microbial characterization

Feiyue Qian[1] · Abebe Temesgen Gebreyesus[1] · Jianfang Wang[1] · Yaoliang Shen[1] · Wenru Liu[1] · Lulin Xie[1]

Received: 19 October 2017 / Revised: 26 December 2017 / Accepted: 5 January 2018 / Published online: 20 January 2018

Abstract

For the possible highest performance of single-stage combined partial nitritation/anammox (PNA) process, a continuous complete-mix granular reactor was operated at progressively higher nitrogen loading rate. The variations in bacterial community structure of granules were also characterized using high-throughput pyrosequencing, to give a detail insight to the relationship between reactor performance and functional organism abundance within completely autotrophic nitrogen removal system. In 172 days of operation, a superior total nitrogen (TN) removal rate over 3.9 kg N/(m^3/day) was stable implemented at a fixed dissolved oxygen concentration of 1.9 mg/L, corresponding to the maximum specific substrate utilization rate of 0.36/day for TN based on the related kinetics modeling. Pyrosequencing results revealed that the genus *Nitrosomonas* responsible for aerobic ammonium oxidation was dominated on the granule surface, which was essential to offer the required niche for the selective enrichment of anammox bacteria (genus *Candidatus* Kuenenia) in the inner layer. And the present of various heterotrophic organisms with general functions, known as fermentation and denitrification, could not be overlooked. In addition, it was believed that an adequate excess of ammonium in the bulk liquid played a key role in maintaining process stability, by suppressing the growth of nitrite-oxidizing bacteria through dual-substrate competitions.

Keywords Partial nitritation · Anammox · Granular sludge · Microbial community structure · Substrate competition

Introduction

As a completely autotrophic nitrogen removal process, combined partial nitritation and anaerobic ammonium oxidation (anammox), PNA for short, is a cost-effective alternate to conventional full nitrification/denitrification for treating ammonium-rich effluent (Van Hulle et al. 2010) and has an application prospect to combine with new energy technologies (such as microbial fuel cell) for achieving sustainable and energy-positive wastewater treatment (Zhang et al. 2014a; Ali and Okabe 2015). In PNA process, aerobic ammonium-oxidizing bacteria (AOB) oxidize part of the influent ammonium to nitrite, and nearly equimolar mixtures of ammonium and nitrite are subsequently converted to dinitrogen gas and small amounts of nitrate by anammox bacteria (AMX) in the absence of oxygen. The overall stoichiometry of PNA process was shown in Eq. 1, with the biomass terms of $C_5H_{1.4}O_{0.4}N_{0.2}$ and $CH_2O_{0.5}N_{0.15}$ representing the growth of AOB and AMX, respectively (Vlaeminck et al. 2012).

$$\begin{aligned} NH_4^+ + 0.792\ O_2 + 0.080\ HCO_3^- \rightarrow & 0.435\ N_2 + 0.111\ NO_3^- \\ & + 0.052\ C_5H_{1.4}O_{0.4}N_{0.2} + 0.028\ CH_2O_{0.5}N_{0.15} \\ & + 1.460\ H_2O + 1.029H^+ \end{aligned} \quad (1)$$

It was well-proven that the PNA process could be implemented in either single-stage or separate-stage bioreactors. Compared to the separate-stage PNA systems, the single-stage ones could offer the prospect of smaller reactor footprint, lower AMX inhibition risk by high nitrite concentration, and less N_2O emissions, but exhibit a higher operational

Feiyue Qian and Abebe Temesgen Gebreyesus contributed equally to this work.

Electronic supplementary material The online version of this article (https://doi.org/10.1007/s00253-018-8768-0) contains supplementary material, which is available to authorized users.

✉ Jianfang Wang
wjf302@163.com

[1] School of Environmental Science and Engineering, Suzhou University of Science and Technology, No. 1 Kerui Road, 215009 Suzhou, People's Republic of China

complexity (Van Hulle et al. 2010; Lackner et al. 2014; Dosta et al. 2015). Typically, the single-stage PNA system is based on biofilm or granular reactor, which could confer the required niche differentiation for enriching key functional organisms, especially slow-growing AMX (Cho et al. 2011; Gilbert et al. 2015; Qian et al. 2017a). For these bioreactors, strict process control of operation conditions such as dissolved oxygen (DO) concentration is essential to achieve the nitrogen removal rate (NRR) ranging from 0.14 to 2.57 kg N/(m^3/day) (Wang et al. 2012; Zhang et al. 2014b; Varas et al. 2015; Wang et al. 2017). On one hand, a sufficient oxygen supply by high aeration intensity could enhance the activity of AOB situated on the biofilm or granule surface and promote the anammox reaction with a high nitrite production (Wang et al. 2014). On the other hand, excessive DO would not only inhibit AMX in the anaerobic functional zone but also favor the growth of undesired nitrite-oxidizing bacteria (NOB), as the competitor with both types of ammonium oxidizers for their electron acceptors (Ma et al. 2015). Thus, in the pursuit of the possible highest performance of single-stage PNA bioreactor, the major challenges are to assure an efficient synergy between AOB and AMX and maintain an adequate selection pressure for NOB.

From a practical perspective, knowledge on the relationship between operation control of bioreactor and microbial community structure in the sludge could contribute to performance optimization and process stability of biological treatment systems. In this study, the performance of a continuous complete-mix granular reactor (CSTR) for single-stage PNA process was dramatically improved by stepwise increasing nitrogen loading rates (NLRs), as evaluated by both biomass growth modeling and substrate utilization kinetics. The development of all bacterial communities in the granules was also characterized using high-throughput pyrosequencing that provided a comprehensive analysis of the relative abundance of bacterial phylotypes within the system. The results obtained were expect to offer convincing explanations for the selection and enrichment mechanisms of different functional organisms and lead to a better understanding of their ecological roles and potential effects on the performance of the bioreactor.

Materials and methods

Reactor setup and operation strategy

A lab-scale CSTR with a working volume of 1.7 L and a settling zone of 0.6 L was installed, in which an approximate complete mix was achieved by combining aerating and hydraulic circulating, as shown in Fig. S1. The temperature and pH value were maintained at 30 ± 1 °C using a water bath and 7.7 ± 0.2 with sufficient alkalinity, respectively. The airflow rate was set at in the range of 0.8 to 2.0 L/min to achieve the oxygen supply.

The reactor was inoculated with pre-acclimated PNA granular sludge with a mixed liquor volatile suspended solids (MLVSS) concentration of around 3800 mg/L, and the biomass with brownish-red showed a compact and spherical-shaped structure and mean size of 0.9 mm, as reported by Qian et al. (2017a). Throughout the entire operation period, the granules represented more than 97% of biomass in CSTR, and the effluent concentration of suspend solid (SS) was always lower than 15 mg/L. Because the biomass was not withdrawn apart from sludge sampling, the sludge retention time (SRT) varying from 35 to 48 days was applied.

The reactor was operated with synthetic media, whose composition (mg/L) was as follows: 1000–3000 $NaHCO_3$, 8.8 KH_2PO_4/11.2 K_2HPO_4 (as PO_4^{3-}-P basis), 20.0 Na_2EDTA, 10.0 $MgSO_4$, 0.1 $FeCl_3{\cdot}6H_2O$, 0.1 $CaCl_2{\cdot}2H_2O$, 0.015 H_3BO_3, 0.015 $CoCl_2{\cdot}6H_2O$, 0.01 $MnCl_2{\cdot}4H_2O$, 0.01 $ZnSO_4{\cdot}7H_2O$, 0.005 $NaMoO_4{\cdot}2H_2O$, 0.003 $CuSO_4{\cdot}5H_2O$, 0.003 KI, and NH_4Cl at required concentration. The pH was adjusted to 7.5–7.8 by adding 10% NaOH solution.

Three different operational stages (I–III) were conducted in 172 days, and the volumetric NLR as NH_4^+-N was initially set at 2.5 kg N/(m^3/day), and finally reached 4.9 kg N/(m^3/day) by stepwise increase in the influent NH_4^+-N concentration corresponding to reactor HRT, as shown in Table 1.

Analytical methods and calculations

The concentrations of MLVSS, SS, NH_4^+-N, NO_2^--N, NO_3^--N, and TN were measured using the procedure described in Standard Methods (APHA 1998). Both solution pH and DO concentration were on-line monitored with PB-10 (Sartorius, Germany) and H1946N portable meters (WTW, Germany), respectively. The granules were sampled regularly and sieved into five size fractions with opening sizes of 0.2, 0.5, 0.8, 1.25, and 1.6 mm, while their mean diameter was equal to the sum of products of weight fractions and the average size in intervals. The granule morphology was observed using a CX41 optical microscope (Olympus, Japan).

As described in our previous study (Qian et al. 2017a), the NH_4^+-N and TN removal efficiencies were calculated on the basis of the difference between corresponding nitrogen concentrations in the influent and effluent, respectively, and the calculation of the NO_3^--N production to remove unit mass of NH_4^+-N as $f(NO_3^-\text{-N}/NH_4^+\text{-N})$ was also performed. The nitrite accumulation percent (NAP) equaled to the concentration ratio of NO_2^--N/(NO_2^--N + NO_3^--N) in the effluent. And the NRR was estimated by calculating the NH_4^+-N and TN removal in the unit reactor volume per day. The food-to-microorganism (F/M) value and the specific nitrogen removal

Table 1 Description of the different operation phases throughout the experiment

Stage	Time (day)	Influent NH_4^+-N concentration (mg/L)	Hydraulic retention time (h)	Nitrogen loading rate (kg N/(m^3/day))
I	1–41	116.9 ± 8.2	1.1	2.5
II	42–83	From 133.3 ± 9.9 to 194.0 ± 5.8	1.1	2.9–4.7
III	84–172	From 217.5 ± 2.0 to 304 ± 12.4	1.5	3.5–4.9

rate (sNRR) were obtained by dividing the MLVSS concentration into NLR and NRR, respectively.

Modeling description

Being similar to bacterial proliferation during batch culture, the biomass growth in CSTR could be simulated or predicted using Sigmoidal nonlinear regression models, as the following expression (Chen et al. 2015):

$$MLVSS(t) = \frac{MLVSS_{\max}}{1 + \exp(-k_1(t - t_0))} \quad (2)$$

where t is the operating time (day), MLVSS(t) is the biomass concentration at t (mg/L), $MLVSS_{max}$ is the maximum biomass concentration expected (mg/L), k_1 is the specific growth rate (1/day), and t_0 is the lag time (day) for biomass increase.

In addition, a mass balance could be performed on nitrogen compounds, showing the mass of NH_4^+-N or TN per unit of time as it enters, exits, accumulates, and reacts in the reactor. It could be given below (Mines 2014):

$$[accumulation] = [inputs] - [outputs] + [reaction] \quad (3)$$

Under pseudo-steady-state conditions, the accumulation term in CSTR was set equal to zero in Eq. 3, and assuming that substrate utilization can be described by Monod model (Shi et al. 2010). Thus, the mass balance was performed as follows:

$$0 = QS_0 - QS_t - \left(\frac{k_2 X S_t}{K_s + S_t}\right) V \quad (4)$$

$$(S_0 - S_t)(K_s + S_t) = k_2 X S_t \tau \quad (5)$$

where S_0 and S_t are the NH_4^+-N or TN concentration in the influent and effluent during the operation, respectively (mg/L); Q is the volumetric inflow rate (m^3/day); k_2 is maximum specific substrate utilization rate (1/day); X is the concentration of MLVSS in CSTR (mg/L), estimated using Eq. 2; V is the working volume of CSTR (m^3); K_S is the half-saturation coefficient of biomass for NH_4^+-N (mg/L). According to the related literatures, the typical K_S value for NH_4^+-N of AOB and AMX were 0.5–1.0 mg/L (Grady et al. 2011) and below 0.1 mg/L (Oshiki et al. 2016), respectively. In this study, K_S was estimated at 0.1 mg/L. τ is the HRT of CSTR (day).

DNA extraction, PCR, and pyrosequencing

The representative granule samples were collected on days 5 and 165 for the purpose of microbial community characterization, respectively. High-throughput pyrosequencing procedure followed Wang et al. (2016), which was performed on the Illumina Miseq platform (Illumina, USA) at Majorbio Bio-Pharm Technology Co., Ltd., Shanghai, China.

Considering the compact structure of granules with abundant extracellular polymeric substance (EPS), the genomic DNA extracted from raw sludge samples ($S5_{sur}$ and $S165_{sur}$), using E.Z.N.A.® Soil DNA Isolation Kit (Omega Bio-tek, Inc., USA) would only represent the microbe distributed in the outer layers of granules. Besides, the slurry of each sludge sample was prepared by ultrasound at 1 W/ml for 10 min in ice bath, and the extracted DNA ($S5_{all}$ and $S165_{all}$) using the same kit represented the overall microbial community in granules. Primer pairs 338F (5′-ACTC CTACGGGAGGCAGCA-3′) and 806R (5′-GGAC TACHVGGGTWTCTAAT-3′) were chosen for the amplification of the V3–V4 regions of the 16S rRNA gene of bacteria. Polymerase chain reaction (PCR) amplifications were carried out in triplicate for each sample using 20 μL reaction mixtures, while the conditions were the following: preheating at 95 °C for 3 min; 27 cycles consisting of denaturation at 95 °C for 30 s, 55 °C annealing for 30 s, and 72 °C for 45 s extension; 10 min at 72 °C of final extension. Combined PCR products were purified and quantified as recommended, prior to pyrosequencing process.

Then, chimeric sequences were identified and removed using UCHIME. Eventually, the numbers of high-quality sequences were 32,656 ($S5_{all}$), 26,214 ($S5_{sur}$), 29,819 ($S165_{all}$), and 26,083 ($S165_{sur}$) with an average length of 442 bp. Raw sequence data had been deposited in the NCBI Sequence Read Archive database (accession number SRP117772). Operational taxonomic units (OTUs) were clustered with 97% similarity cutoff using UPARSE embedded in Qiime, and the most abundant sequences in OTUs were assigned to taxonomic classifications by the Ribosomal Database Project (RDP) Classifier with a confidence threshold of 70%. In

addition, the alpha diversity analysis including rarefaction curves, species richness estimators of Chao1 and ace, Shannon and Simpson diversity indexes, and abundance-based coverage were conducted. The approximately maximum-likelihood phylogenetic tree of 16S rRNA gene sequences was constructed using FastTree version 2.1.3 (http://www.microbesonline.org/fasttree/).

It should be noted that the archaea community analysis was also conducted following the similar procedure, in which the primers employed were Arch334F (5′-ACGG GGYGCAGCAGGCGCGA-3′) and Arch915R (5′-GTGC TCCCCCGCCAATTCCT-3′) instead (Qian et al. 2017b). Results revealed that the genera *Halobacteriales*, *Halobacteriaceae*, *Halobacterium*, and *Euryarchaeota* dominated in the granules, while there were no typical ammonia-oxidizing archaea detected (data not shown).

Results

Reactor performance and sludge morphology

In stage I (days 1–41), the CSTR was operated at the NLR of 2.5 kg N/(m^3/day). For the first 22 days, the aeration flow rate was set at 0.8 L/min, corresponding to a DO level of 1.6 mg/L. As depicted in Fig. 1, the average removal efficiencies of NH_4^+-N and TN were 68.5 ± 4.7 and 57.1 ± 3.3% from day 10 to day 22, respectively. Meanwhile, NO_2^--N concentration in the effluent (5.2 ± 0.8 mg/L) was only 1/7 of the residual NH_4^+-N concentration (36.7 ± 5.6 mg/L), indicating that the ammonium oxidation to nitrite could be the rate-limiting step for PNA process. From day 23, the DO concentration in CSTR was slightly increased to 1.9 mg/L by adjusting the aeration flow rate. Consequently, both NH_4^+-N and TN removal were considerably enhanced. On day 41, the NH_4^+-N and TN removal reached 98.4 and 82.3%, respectively, and the effluent NAP was around 30%. With completely autotrophic medium in the influent, the $f(NO_3^-\text{-N}/NH_4^+\text{-N})$ was calculated at 0.10 ± 0.02, almost identical with the stoichiometric value of 0.11 on the basis of Eq. 1. It indicated the nitrate in the effluent was mainly produced through PNA process, instead of nitrite oxidation by NOB.

In the following stage (days 42–83), the influent NH_4^+-N concentration was increased stepwise once the NH_4^+-N removal over 95% was achieved; this resulted in a steady increase of NLR from 2.9 to 4.7 kg N/(m^3/day) throughout this stage. The DO concentration was maintained at 1.9 mg/L with the required aeration flow rate. It showed several fluctuations in the performance of reactor, and the NRR briefly increased to 3.7 kg N/(m^3/day) on day 82, 2.7 times higher than the value of 1.0 kg N/(m^3/day) at the beginning of stage I. However, huge nitrogen gas production as the result of the high NRR caused a heavy sludge floating in the upper part

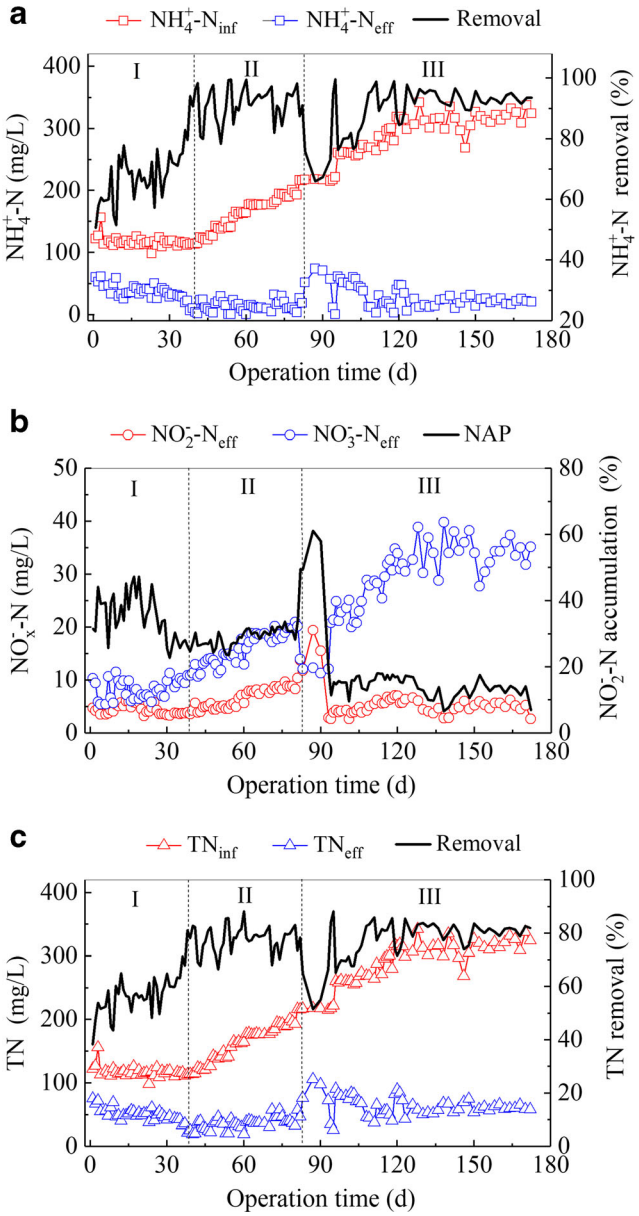

Fig. 1 Changes in **a** NH_4^+-N removal, **b** NO_x^--N production, and **c** TN removal in the CSTR throughout the operation period (phases I–III)

of the settling zone on day 83, and only a small portion of biomass was retained in the reaction zone. The sharp decrease in the NH_4^+-N and TN removal suggested that the CSTR could not support a NLR as 4.7 kg N/(m^3/day) under this condition. For these reasons, the HRT of reactor was extended to 1.5 h from day 84, resulting in the decrease of NLR to kg N/(m^3/day). According to Li et al. (2014), the floated sludge was centrifuged at a 8000g-force for 5 min and the pellets were put back to the CSTR, in order to release gaseous product and improve the settling ability of granules.

After 10 days of operation, the performance of CSTR was effectively restored, with the 94.8% NH_4^+-N and 84.0% TN removal on day 94. The further increase in the influent NH_4^+-

N concentration from around 220 to over 300 mg/L was implemented from day 95 to day 124, while the DO level was fixed at 1.9 mg/L by enhancing the aeration intensity simultaneously. Although the increase of NLR to 4.9 kg N/(m^3/day) had a short-term negative impact on the reactor performance, the NH_4^+-N and TN removal would be higher than 90 and 80% from day 124, respectively. Because the corresponding aeration flow rate of 2 L/min was so great to give a high risk of sludge washout, the CSTR was run at the NLR of 4.9 kg N/(m^3/day) to evaluate the stability of autotrophic nitrogen removal process. It was noteworthy that high-speed centrifugation for the floated granules was also used in this period, to minimize sludge loss with the effluent. As illustrated in Fig. 1, the average NH_4^+-N and TN removal were 93.3 ± 2.0 and 80.9 ± 2.6% from day 125 to day 172, respectively. A NRR over 3.9 kg N/(m^3/day) with the $f(NO_3^-$-N/NH_4^+-N) of 0.12 ± 0.01 could prove that a highly efficient single-stage PNA process had been started up.

In addition, Fig. S2 showed the particle size distributions and morphology of the granules at different operational stages. It indicated that a higher NLR would not bring a significant increase in the mean size of granules, stabilizing at around 0.97 mm; however, the dominant size fraction was changed from 0.5–0.8 mm (49.5% on day 5) to 0.8–1.25 mm (42.3% on day 165). And the mature granules had a compact near-spherical shape with a smooth profile, in which a dense and reddish inner core was surrounded by a gelatinous and brown rim.

Biomass growth and substrate utilization modeling

Without discharging residual sludge, a progressive growth of biomass was observed in Fig. 2, which resulted in the decrease of F/M value from 0.61 ± 0.03 g N/(g VSS·day) in stage I and II to 0.53 ± 0.02 g N/(g VSS·day) in stage III. And Sigmoidal model fitted the biomass growth with the operation time of CSTR very well (R^2 = 0.9677). According to Eq. 6, a low specific growth rate of k_1 = 0.017/day for granules was expected under completely autotrophic condition, with a quite long lag time of t_0 = 54 day. More importantly, it indicated that the exact biomass could be estimated at any t, even if the biomass analysis was not conducted:

$$MLVSS(t) = \frac{11184.86}{1 + \exp(-0.01656(t-54.06))} \quad (6)$$

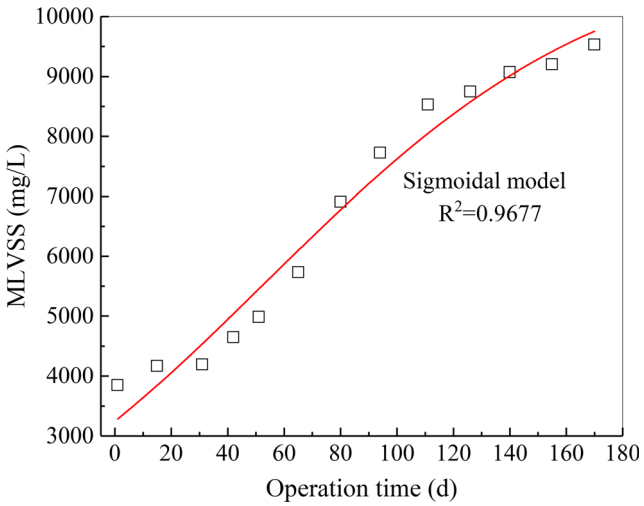

Fig. 2 Simulation of the biomass growth of granules in CSTR during the operation

Figure 3a, b showed the graph plotted between $(S_0\text{-}S_t)(K_s + S_t)$ against $XS_t\tau$, on the basis of the operational results of stage II to III in this study, and the linear regressions were also performed with the experimental data of nitrogen removal operation in similar granular reactors reported by other researchers (Fig. 3c–f). It revealed that the data containing high correlation ($R^2 > 0.97$) was applied to the model. According to Eq. 5, k_2 values for NH_4^+-N and TN were obtained from the slope of the lines.

In previous reports, the sNRRs were widely used to represent the activities of functional organisms in the granules and analyze the variations in bioreactor performance (Vlaeminck et al. 2010; Chu et al. 2015; Varas et al. 2015). However, numerous operational conditions, such as substrate composition, DO level, temperature, reaction volume, biomass, sludge morphology, and even operating time, could have considerable influences on the sNRR estimation, whether in situ or ex situ methods were employed (Vázquez-Padín et al. 2010; Ke et al. 2015). These make it difficult to conduct an objective comparison among the sNRRs in different studies. As demonstrated in Table 2, increasing the applied NLR resulted in the sNRR values as NH_4^+-N and TN varying in a certain range, while a special k_2 value was in accordance with the sNRR level of granules. It was believed that substrate utilization modeling provides a more reliable approach for characterizing differentiation in bioreactor performance, given that k_2 value was obtained from long-term operational data.

Microbial community structure analysis

High-throughput pyrosequencing was applied to analyze the bacterial community structure of four samples, including $S5_{all}$, $S5_{sur}$, $S165_{all}$, and $S165_{sur}$, and there were a total of 494 different OTUs sharing 97% identity in the granules. As summarized in Table 3, the coverage estimators of samples were higher than 99.7%, and rarefaction curves (Fig. S3) approaching an asymptote suggested that the sequencing depth was well enough to represent the whole diversity. Comparing to the granules ($S5_{all}$) at low NLR,

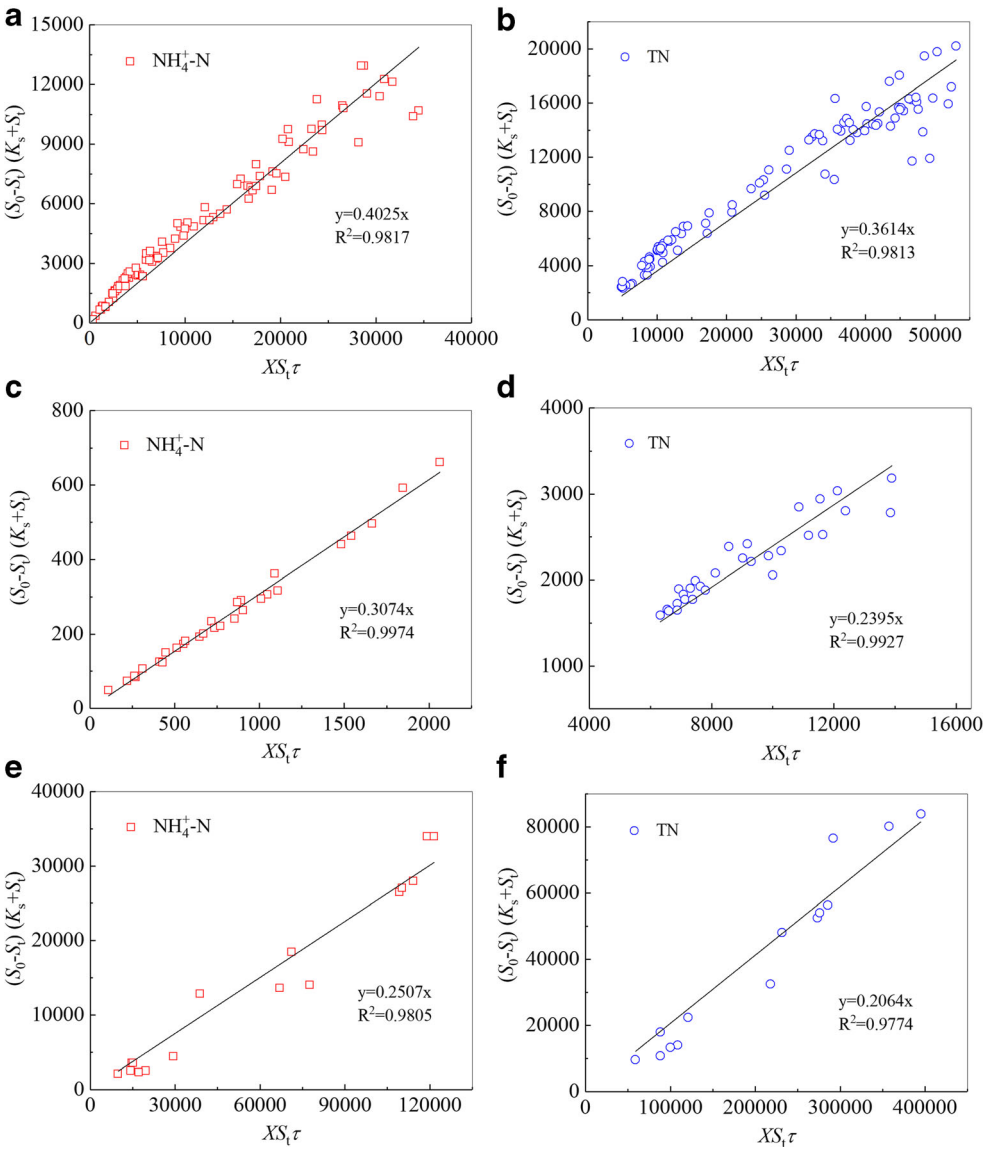

Fig. 3 Simulation of NH_4^+-N and TN removal in CSTR, based on the results in this study (**a**, **b**) and reported by Qian et al. (2017a) (**c**, **d**) and Wang et al. (2017) (**e**, **f**)

both bacterial richness and diversity of $S165_{all}$ decreased slightly. But, a reverse phenomenon for the bacterial community in the outer layer of the granules ($S5_{sur}$ and $S165_{sur}$) was observed.

The shared and unique OTUs in the four samples are illustrated in Fig. 4a, and the identification of bacterial communities for each sample on three different taxonomic levels, including phylum (a total of 28), class (60), and genus (236), are also illustrated in Fig. 4b–d, respectively. Figure 5 showed the phylogenetic affiliation of top 40 abundant genera in the granules.

For $S5_{all}$, *Proteobacteria* was the most abundant phylum with a relative abundance of 34.5%, followed by *Chloroflexi* (20.3%), *Planctomycetes* (17.5%), *Bacteroidetes* (15.4%),

Table 2 Comparisons of substrate utilization kinetic values of different PNA granules in CSTR

No.	Nitrogen loading rate (kg N/(m^3/day))	Specific nitrogen removal rates (g N/(g VSS·day))		k_2 value (1/day)		Reference
		NH_4^+-N	TN	NH_4^+-N	TN	
1	2.9–4.9	0.46–0.58	0.41–0.46	0.40	0.36	This study
2	2.7–3.3	0.25–0.28	0.19–0.24	0.31	0.24	Qian et al. (2017a)
3	0.5–2.5	0.13–0.26	0.11–0.23	0.25	0.21	Wang et al. (2017)

Table 3 The observed OTUs and richness/diversity estimators for the four samples

Sample	OTU	Richness index		Diversity index		Coverage (%)
		Chao1	ACE	Shannon	Simpson	
$S5_{all}$	299	349.6	355.3	3.850	0.0500	99.82
$S5_{sur}$	251	310.0	310.9	3.029	0.1251	99.77
$S165_{all}$	302	334.2	335.1	3.206	0.1428	99.84
$S165_{sur}$	253	324.7	321.8	3.118	0.1041	99.75

Ignavibacteriae (4.9%), *Acidobacteria* (2.4%), and *Chlorobi* (1.5%) etc., together accounting for around 96.5% of all the classified sequences (Fig. 4b). Most of these phyla were omnipresent in various types of PNA or anammox bioreactors (Chu et al. 2015; Gonzalez-Martinez et al. 2015a, b; Luo et al. 2017). In addition, there were 184 OTUs shared by $S5_{all}$ and $S165_{all}$, representing over 60% in the two samples (Fig. 4a). *Planctomycetes* (43.3%) became the dominant phylum in $S165_{all}$, instead of *Proteobacteria* (22.7%), while other major ones included *Chloroflexi* (21.2%), *Bacteroidetes* (4.7%), *Acidobacteria* (2.9%), WWE3 (1.3%), and *Chlorobi* (1.0%). In comparison, the 210 shared OTUs revealed a higher similarity between $S5_{sur}$ and $S165_{sur}$. *Proteobacteria* (68.7% in $S5_{sur}$ and 56.8% in $S165_{sur}$) overwhelmingly predominated in the bacterial community on the granule surface, and *Bacteroidetes* (16.8% in $S5_{sur}$ and 12.7% in $S165_{sur}$) made up the second most abundant phylum. In particular, the fractions of phyla *Planctomycetes* and *Nitrospirae* in $S165_{sur}$ reached 11.9 and 5.5%, respectively, corresponding to the values of 3.6 and 1.5% in $S5_{sur}$.

On the class level (Fig. 4c), *Betaproteobacteria* (19.8%), *Planctomycetacia* (17.4%), *Anaerolineae* (15.6%), and *Sphingobacteriia* (10.8%) were the top four abundant taxa in $S5_{all}$, which dominated in phyla *Proteobacteria*, *Planctomycetes*, *Chloroflexi*, and *Bacteroidetes*, respectively. Different from $S5_{all}$, class *Planctomycetacia* represented the 39.3% of all the bacteria in $S165_{all}$, while the fraction of *Betaproteobacteria* decreased to 9.8%. On the granule surface, *Betaproteobacteria* contributed around 50% in the two samples, and the percentage of *Planctomycetacia* rose obviously from 1.8% in $S5_{sur}$ to 9.0% in $S165_{sur}$.

As expected, the co-existence of AOB and AMX were found in the granules as evidence by their bacterial communities on the genus level, while the growth of NOB was

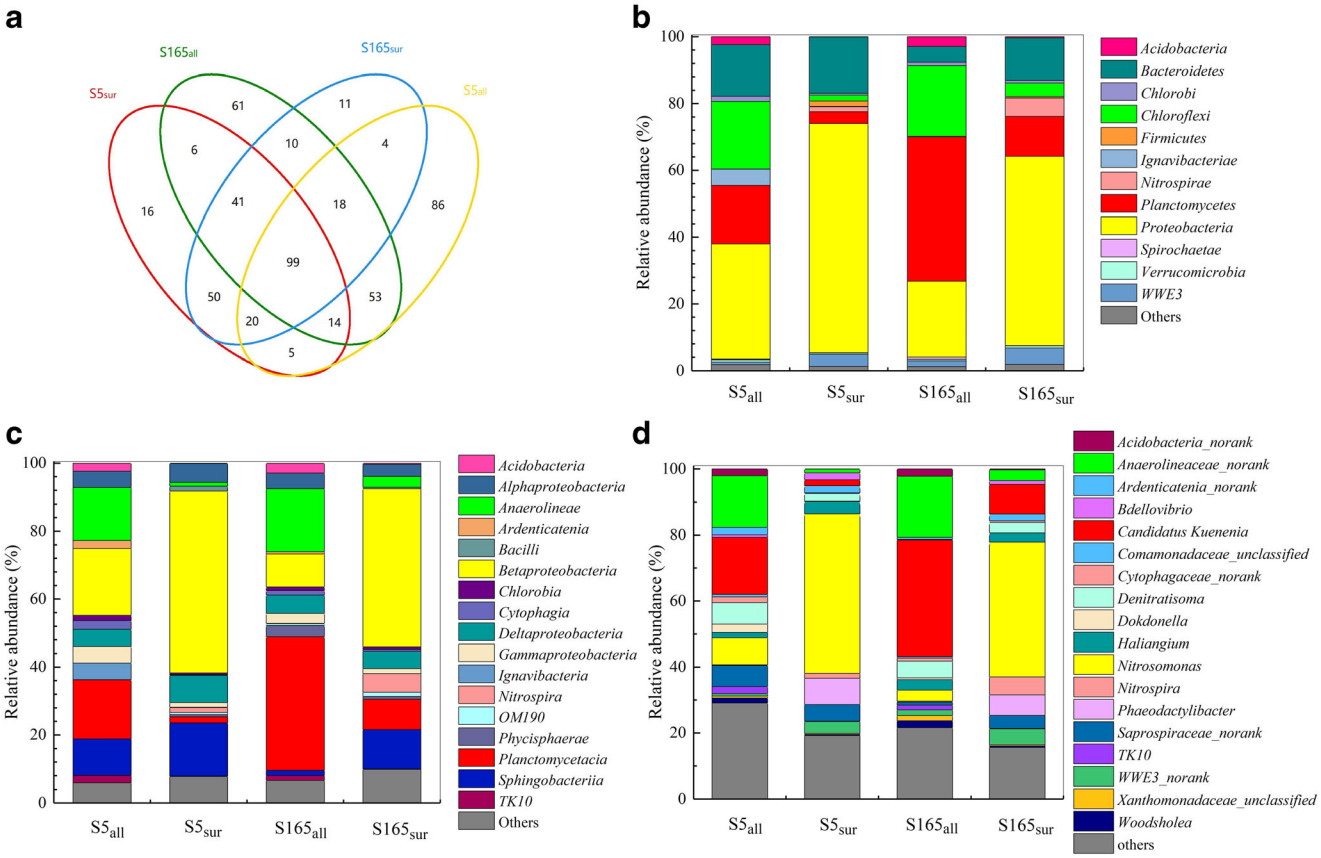

Fig. 4 **a** Venn diagram of shared OTUs (3% distance level) between the four samples and the dominant taxa found in each one, identified to the phylum (**b**), class (**c**), and genus (**d**) level

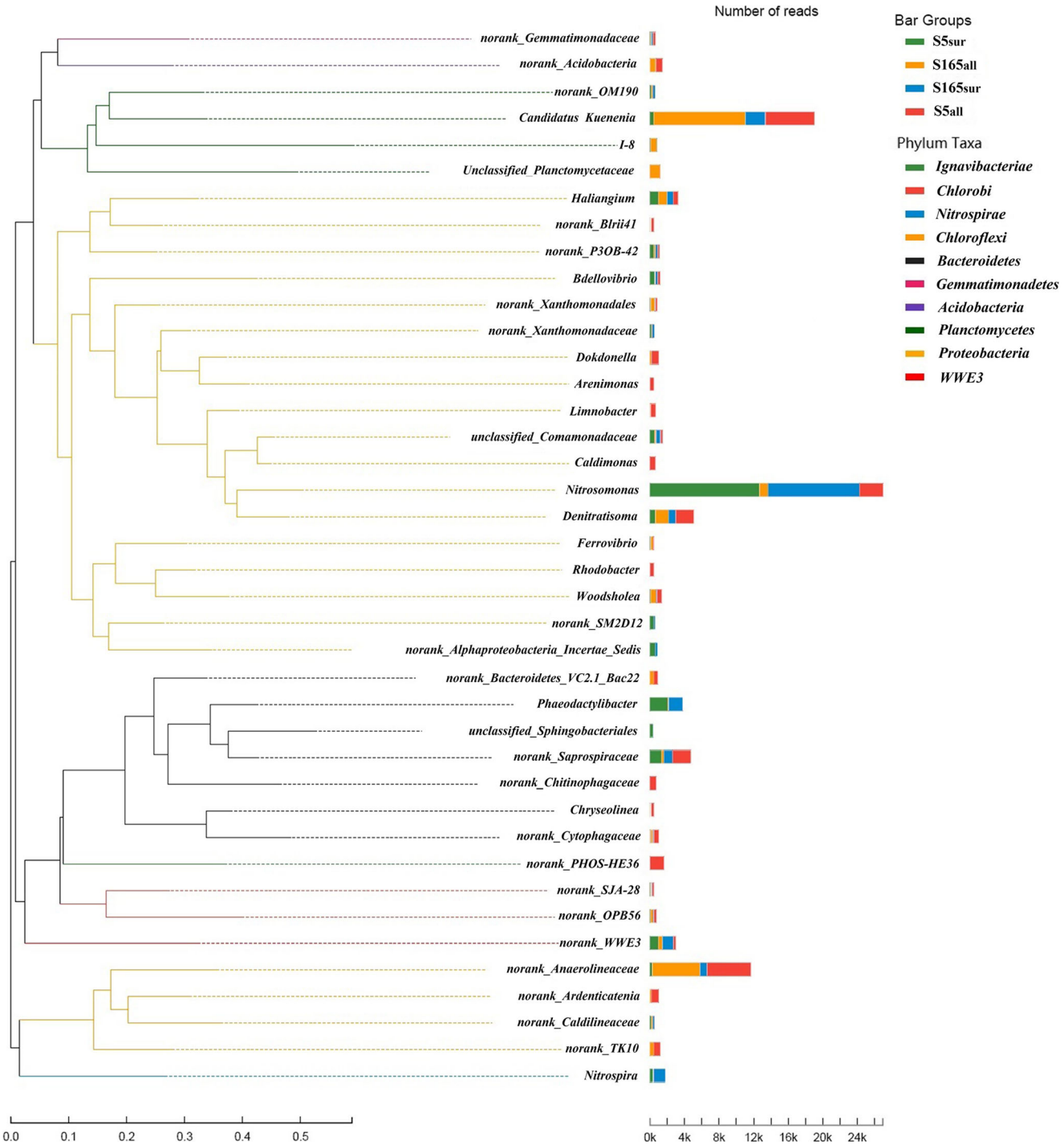

Fig. 5 Phylogenetic tree of top 40 abundant genera in the granules

effectively suppressed (Figs. 4d and 5). Genera *Nitrosomonas* (affiliated to class *Betaproteobacteria*) and *Candidatus* Kuenenia (affiliated to class *Planctomycetacia*) were identified as the main AOB and AMX species, respectively, which closely cooperated and accomplished completely autotrophic nitrogen removal in CSTR. Although the abundance of AOB decreased from 8.1% in $S5_{all}$ to 3.3% in $S165_{all}$ during the operation, *Nitrosomonas* (48.3% in $S5_{sur}$ and 40.8% in $S165_{sur}$) dominated in the total number of bacteria on the granule surface. Considering that the PNA bioreactor is an ammonium-driven ecosystem, the enrichment of AMX (35.4%) in $S165_{all}$ was observed at around two times higher NLR, compared with the AMX fraction of 17.4% in $S5_{all}$. Meanwhile, there were only few *Nitrospira* spp. detected on the granule surface, and the abundance of them (< 0.05%) could be ignored in $S5_{all}$ and $S165_{all}$. Interestingly, there were

various satellite heterotrophic organisms with general functions identified in the granules, revealing a significant biodiversity. As another dominant population besides AOB and AMX in $S5_{all}$ and $S165_{all}$, norank_*Anaerolineaceae* belonging to the phylum *Chloroflexi* was known as the fermentation bacteria, which could grow on the organic products released by autotroph (AOB and AMX) decay in the single-stage PNA systems, and the filamentous members also provided a stabilizing framework for the three-dimensional spatial structure of granules (Cho et al. 2011; Chu et al. 2015). Moreover, the present of *Denitratisoma*, norank_*Acidobacteria*, norank_*Saprospiraceae*, *Dokdonella*, and unclassified_*Xanthomonadaceae* etc. with relatively low abundances of 0.6~6.5% were also observed (Figs. 4d and 5), and some of them were considered to have the capability of anoxic nitrate or nitrous oxide reduction through heterotrophic metabolism (Cho et al. 2011; Gonzalez-Gil et al. 2015; Gonzalez-Martinez et al. 2015a, b).

Discussion

The mechanisms of efficient nitrogen removal based on granules

This study gives a detailed insight into the reactor performance, substrate utilization kinetics, and bacterial community structure of the granules in a single-stage PNA system. During the operation, the NLR was progressively increased from 2.5 to 4.9 kg N/(m^3/day) with a high aeration intensity in CSTR, resulting in the superior k_2 values of 0.40/day for NH_4^+-N and 0.36/day for TN, respectively. The dense granules could offer the required ecological niches for different functional organisms, by means of a steep substrate gradient within them (Vázquez-Padín et al. 2010; Vlaeminck et al. 2010).

As illustrated in Figs. 4d and 5, a typical AOB (genus *Nitrosomonas*) rim was situated in the outer layer of granules, where partial nitritation step was accomplished to produce the sufficient nitrite for anammox reaction, and to consume the available oxygen for creating anoxic environment in the inner layer. *Nitrosomonas* spp. have been widely reported as ammonium oxidizers in the single-stage PNA systems and hold high growth rate and activity at oxygen and ammonium-rich conditions as *r*-strategist, which allows them to outcompete other AOB such as *Nitrosospira* sp. on the granule surface (Chu et al. 2015; Gonzalez-Martinez et al. 2015b). Usually, an oxygen-limited control strategy is implemented in a single-stage PNA system using intermittent or low-strength aeration, to avoid AMX inhibition by excessive DO (Zhang et al. 2014b; Hubaux et al. 2015; Zheng et al. 2016). In this study, a stable TN removal around 80% in CSTR was achieved, although the applied DO concentration of 1.6–1.9 mg/L was much higher than the typical ones of 0.1–0.6 mg/L in other continuous bioreactors (Varas et al. 2015; Li et al. 2016b; Wang et al. 2017). According to our previous study (Qian et al. 2017a), there was a significant positive correlation between sNRR values and EPS contents in the granules. It might be argued that high EPS contents played an important role in the anaerobic niche construction for AMX by increasing oxygen penetration resistance (Vlaeminck et al. 2010; Zheng et al. 2016). For these reasons, the abundance of *Candidatus* Kuenenia on the granule surface was also increased from 1.8% in $S5_{sur}$ to 9.0% in $S165_{sur}$, which were close to the bulk liquid and AOB rims (Figs. 4d and 5). Further studies on the relationships among EPS contents, granular morphology, and AMX habitat should be conducted for offering more experimental evidences.

As the sole genus responsible for anammox reaction in the granules, *Candidatus* Kuenenia is regarded as *k*-strategist with high substrate affinities and low maximum growth rate, since its half-saturation constant for nitrite (K_S = 0.2–3 μM) is significantly lower than that for the other four AMX genera found in wastewater treatment systems, including Brocadia, Jettenia, Anammoxoglobus, and Scalindua (Oshiki et al. 2016). In this view, *Ca.* Kuenenia would take competitive advantages in adapting to a nitrite-limiting environment, like single-stage PNA bioreactor in continuous-flow mode (Park et al. 2015; Wang et al. 2017), while *Ca.* Brocadia, *Ca.* Scalindua, and *Ca.* Jettenia prefer to grow in the substrate-rich anammox-based unit (Chu et al. 2015; Gonzalez-Gil et al. 2015; Gonzalez-Martinez et al. 2015a). As shown in Fig. 1, the NO_2^--N concentration in CSTR was much blow 10 mg/L in most time of operation, which could explain the selective enrichment of *Ca.* Kuenenia in the granules.

NOB repression in continuous granular reactor

It was well known that the overgrowth of NOB would certainly deteriorate the overall performance of single-stage PNA system, by means of further oxidizing nitrite to nitrate (Third et al. 2001). As mentioned above, an efficient TN removal with the $f(NO_3^-\text{-N}/NH_4^+\text{-N})$ value of 0.10–0.12 was achieved in CSTR, which was consistent with the extreme low fractions of *Nitrospira* and no *Nitrobacter* detected in the granules ($S5_{all}$ and $S165_{all}$). And, the residual NH_4^+-N in the bulk liquid was determined as the key operational parameter for suppressing NOB growth. On one hand, an adequate excess of NH_4^+-N (Fig. 1) could enhance aerobic ammonium oxidation rate by AOB and assure oxygen-limiting conditions in the inner layer, with the ratio between DO and NH_4^+-N concentrations lower than 0.2 mg/mg, which was beneficial to washout the NOB having lower oxygen affinity than AOB, such as *Nitrobacter* (Jemaat et al. 2014; Poot et al. 2016). However, it might not work well in the repression of *Nitrospira*, due to its anaerobic or microaerophilic origin (Regmi et al. 2014). On the other hand, the residual NH_4^+-N was essential to maintain the effluent NO_2^--N concentration on limited level by enhancing AMX activity (Pérez et al. 2014). The difference in nitrite affinity between AMX and NOB offered an assistant selection pressure

for the latter, because the *K*s values of *Nitrobacter* and *Nitrospira* (49–544 and 9–27 μM respectively) are much higher as compared to *Ca.* Kuenenia (Nowka et al. 2015). Thus, the dual competition of common substrates among three functional organisms would be the main mechanism for achieving the out-selection of NOB from the granules.

The potential functions of satellite heterotrophs in granules

Despite a very simple composition of the inorganic influent of CSTR, the autotrophic nitrogen removal process with a long SRT triggered various secondary reactions by versatile heterotrophs in the granules, as similar to that that took place in industrial anammox-based systems (Gonzalez-Martinez et al. 2015b; Luo et al. 2017). Based on the functions derived from the draft genome, Speth et al. (2016) proposed an ecological model of the biological nitrogen cycle in a full-scale single-stage PNA bioreactor, suggesting that partial denitrification and nitrogenous intermediates transfer could play an important role in the system. The similar results were also obtained from several anammox granular reactors (Gonzalez-Gil et al. 2015; Guo et al. 2016). In this view, the fermentation of complex microbial products from biomass decay were conducted by functional organisms, such as members within *Chloroflexi* and *Ignavibacterium*, which provided readily biodegradable organics to heterotrophic denitrifiers, like some of *Proteobacteria*, *Chlorobi*, and *Acidobacteria* etc. Unfortunately, the contribution of denitrification to the TN removal in CSTR was negligible, as evidenced by a typical $f(NO_3^-\text{-N}/NH_4^+\text{-N})$ value for completely autotrophic nitrogen removal process throughout the entire operation period, due to the limited carbon supply by the organics fermentation as sole source. It could be expected that the produced nitrate by anammox reaction is partly or totally reduced to nitrite as the AMX substrate for further improving effluent quality, while a simultaneous nitritation, anammox, and denitrification (SNAD) process was developed, by optimizing operational conditions such as NLR, COD/TN ratio, and aeration mode of the bioreactor etc. (Gonzalez-Gil et al. 2015; Zhang et al. 2015; Li et al. 2016a). In the future, the microbial ecology and community functioning of single-stage PNA bioreactor should be studied in depth using genome-resolved metagenomics, meta-transcriptomics and meta-proteomics, considering that the definite correlation between organism abundance and activity was not always found in complex biological systems (Speth et al. 2016).

Acknowledgements This study was supported by the National Natural Science Foundation of China (51308367, 51578353) and the Natural Science Foundation of Jiangsu Province, China (BK20150284). The authors also acknowledge support from the Preponderant Discipline Construction Project in higher education of Jiangsu Province, China, and the Two-year International Master Program on Environmental Engineering authorized by the Chinese Ministry of Commerce (2015E0434).

Compliance with ethical standards

Ethical statement This article does not contain any studies with human participants or animals performed by any of the authors.

Conflict of interest The authors declare that they have no conflict of interest.

References

Ali M, Okabe S (2015) Anammox-based technologies for nitrogen removal: advances in process start-up and remaining issues. Chemosphere 141: 144–153. https://doi.org/10.1016/j.chemosphere.2015.06.094

APHA (1998) Standard methods for examination of water and wastewater, 20th edn. American Public Health Association, New York

Chen FY, Liu YQ, Tay JH, Ning P (2015) Rapid formation of nitrifying granules treating high-strength ammonium wastewater in a sequencing batch reactor. Appl Microbiol Biotechnol 99(10):4445–4452. https://doi.org/10.1007/s00253-014-6363-6

Cho S, Fujii N, Lee T, Okabe S (2011) Development of a simultaneous partial nitrification and anaerobic ammonia oxidation process in a single reactor. Bioresour Technol 102(2):652–659. https://doi.org/10.1016/j.biortech.2010.08.031

Chu ZR, Wang K, Li XK, Zhu MT, Yang L, Zhang J (2015) Microbial characterization of aggregates within a one-stage nitritation–anammox system using high-throughput amplicon sequencing. Chem Eng J 262:41–48. https://doi.org/10.1016/j.cej.2014.09.067

Dosta J, Vila J, Sancho I, Basset N, Grifoll M, Mata-Álvarez J (2015) Two-step partial nitritation/Anammox process in granulation reactors: start-up operation and microbial characterization. J Environ Manag 164: 196–205. https://doi.org/10.1016/j.jenvman.2015.08.023

Gilbert EM, Agrawal S, Schwartz T, Horn H, Lackner S (2015) Comparing different reactor configurations for partial nitritation/anammox at low temperatures. Water Res 81:92–100

Gonzalez-Gil G, Sougrat R, Behzad AR, Lens PN, Saikaly PE (2015) Microbial community composition and ultrastructure of granules from a full-scale anammox reactor. Microb Ecol 70(1):118–131. https://doi.org/10.1007/s00248-014-0546-7

Gonzalez-Martinez A, Osorio F, Rodriguez-Sanchez A, Martinez-Toledo MV, Gonzalez-Lopez J, Lotti T, van Loosdrecht MCM (2015a) Bacterial community structure of a lab-scale anammox membrane bioreactor. Biotechnol Prog 31(1):186–193. https://doi.org/10.1002/btpr.1995

Gonzalez-Martinez A, Rodriguez-Sanchez A, Muñoz-Palazon B, Garcia-Ruiz MJ, Osorio F, van Loosdrecht MCM, Gonzalez-Lopez J (2015b) Microbial community analysis of a full-scale DEMON bioreactor. Bioprocess Biosyst Eng 38(3):499–508. https://doi.org/10.1007/s00449-014-1289-z

Grady CPL, Daigger GT, Love NG, Filipe CDM (2011) Biological wastewater treatment, 3rd edn. CRC Press, London, pp 99–102

Guo JH, Peng YZ, Fan L, Zhang L, Ni BJ, Kartal B, Feng X, Jetten MSM, Yuan ZG (2016) Metagenomic analysis of anammox communities in three different microbial aggregates. Environ Microbiol 18(9): 2979–2993. https://doi.org/10.1111/1462-2920.13132

Hubaux N, Wells G, Morgenroth E (2015) Impact of coexistence of flocs and biofilm on performance of combined nitritation-anammox granular sludge reactors. Water Res 68:127–139

Jemaat Z, Suárez-Ojeda ME, Pérez J, Carrera J (2014) Partial nitritation and o-cresol removal with aerobic granular biomass in a continuous

airlift reactor. Water Res 48:354–362. https://doi.org/10.1016/j.watres.2013.09.048

Ke Y, Azari M, Han P, Görtz I, Gu JD, Denecke M (2015) Microbial community of nitrogen-converting bacteria in anammox granular sludge. Int Biodeter Biodegr 103:105–115. https://doi.org/10.1016/j.ibiod.2015.04.011

Lackner S, Gilbert EM, Vlaeminck SE, Joss A, Horn H, van Loosdrecht MCM (2014) Full-scale partial nitritation/anammox experiences—an application survey. Water Res 55:292–303. https://doi.org/10.1016/j.watres.2014.02.032

Li JZ, Meng J, Li JL, Wang C, Deng KW, Sun K, Buelna G (2016a) The effect and biological mechanism of COD/TN ratio on nitrogen removal in a novel upflow microaerobic sludge reactor treating manure-free piggery wastewater. Bioresour Technol 209:360–368

Li W, Zheng P, Ji JY, Zhang M, Guo J, Zhang JQ, Abbas G (2014) Floatation of granular sludge and its mechanism: a key approach for high-rate denitrifying reactor. Bioresour Technol 152:414–419. https://doi.org/10.1016/j.biortech.2013.11.056

Li XJ, Sun S, Badgley BD, Sung S, Zhang H, He Z (2016b) Nitrogen removal by granular nitritation-anammox in an upflow membrane-aerated biofilm reactor. Water Res 94:23–31. https://doi.org/10.1016/j.watres.2016.02.031

Luo JH, Chen H, Han XY, Sun YF, Yuan ZG, Guo JH (2017) Microbial community structure and biodiversity of size-fractionated granules in a partial nitritation-anammox process. FEMS Microbiol Ecol 93:1–10

Ma B, Bao P, Wei Y, Zhu GB, Yuan ZG, Peng YZ (2015) Suppressing nitrite-oxidizing bacteria growth to achieve nitrogen removal from domestic wastewater via anammox using intermittent aeration with low dissolved oxygen. Sci Rep 5(1):13048–13057. https://doi.org/10.1038/srep13048

Mines RO (2014) Environmental engineering principles and practice, 1st edn. John Wiley & Sons, Ltd, Chichester

Nowka B, Daims H, Spieck E (2015) Comparison of oxidation kinetics of nitrite-oxidizing bacteria: nitrite availability as a key factor in niche differentiation. Appl Environ Microbiol 81(2):745–753. https://doi.org/10.1128/AEM.02734-14

Oshiki M, Satoh H, Okabe S (2016) Ecology and physiology of anaerobic ammonium oxidizing bacteria. Environ Microbiol 18:2784–2796

Park H, Sundar S, Ma Y, Chandran K (2015) Differentiation in the microbial ecology and activity of suspended and attached bacteria in a nitritation-anammox process. Biotechnol Bioeng 112(2):272–279. https://doi.org/10.1002/bit.25354

Pérez J, Lotti T, Kleerebezem R, Picioreanu C, van Loosdrecht MCM (2014) Outcompeting nitrite-oxidizing bacteria in single-stage nitrogen removal in sewage treatment plants: a model-based study. Water Res 66:208–218

Poot V, Mithell H, Geleijnse MA, van Loosdrecht MCM, Pérez J (2016) Effects of the residual ammonium concentration on NOB repression during partial nitritation with granular sludge. Water Res 106:518–530. https://doi.org/10.1016/j.watres.2016.10.028

Qian FY, Wang JF, Shen YL, Wang Y, Wang SY, Chen X (2017a) Achieving high performance completely autotrophic nitrogen removal in a continuous granular sludge reactor. Biochem Eng J 118:97–104. https://doi.org/10.1016/j.bej.2016.11.017

Qian FY, Chen X, Wang JF, Shen YL, Gao JJ, Mei J (2017b) Differentiation in nitrogen-converting activity and microbial community structure between granular size fractions in a continuous autotrophic nitrogen removal reactor. J Microbiol Biotechnol 27(10):1798–1807. https://doi.org/10.4014/jmb.1705.05042

Regmi P, Miller MW, Holgate B, Bunce R, Park H, Chandran K, Wett B, Murthy S, Bott CB (2014) Control of aeration, aerobic SRT and COD input for mainstream nitritation/denitritation. Water Res 57:162–171. https://doi.org/10.1016/j.watres.2014.03.035

Shi XY, Sheng GP, Li XY, Yu HQ (2010) Operation of a sequencing batch reactor for cultivating autotrophic nitrifying granules. Bioresour Technol 101(9):2960–2964. https://doi.org/10.1016/j.biortech.2009.11.099

Speth DR, in't Zandt MH, Guerrero-Curz S, Dutilh BE, MSM J (2016) Genome-based microbial ecology of anammox granules in a full-scale wastewater treatment system. Nat Commun 7:11172–11182. https://doi.org/10.1038/ncomms11172

Third KA, Sliekers AO, Kuenen JG, Jetten MSM (2001) The CANON system (completely autotrophic nitrogen-removal over nitrite) under ammonium limitation: interaction and competition between three groups of bacteria. Syst Appl Microbiol 24(4):588–596. https://doi.org/10.1078/0723-2020-00077

Van Hulle SWH, Vandeweyer HJP, Meesschaert BD, Vanrolleghem PA, Dejans P, Dumoulin A (2010) Engineering aspects and practical application of autotrophic nitrogen removal from nitrogen rich streams. Chem Eng J 162(1):1–20. https://doi.org/10.1016/j.cej.2010.05.037

Varas R, Guzman-Fierro V, Giustinianovich E, Behar J, Fernandez K, Roeckel M (2015) Startup and oxygen concentration effects in a continuous granular mixed flow autotrophic nitrogen removal reactor. Bioresour Technol 190:345–351. https://doi.org/10.1016/j.biortech.2015.04.086

Vázquez-Padín J, Mosquera-Corral A, Campos JL, Méndez R, Revsbech NP (2010) Microbial community distribution and activity dynamics of granular biomass in a CANON reactor. Water Res 44:4359–4370

Vlaeminck SE, De Clippeleir H, Verstraete W (2012) Microbial resource management of one-stage partial nitritation/anammox. Microb Biotechnol 5:433–448

Vlaeminck SE, Terada A, Smets BF, De Clippeleir H, Schaubroeck T, Bolca S, Demeestere L, Mast J, Boon N, Carballa M, Verstraete W (2010) Aggregate size and architecture determine microbial activity balance for one-stage partial nitritation and anammox. Appl Environ Microbiol 76:900–909

Wang JF, Qian FY, Liu XP, Liu WR, Wang SY, Shen YL (2016) Cultivation and characteristics of partial nitrification granular sludge in a sequencing batch reactor inoculated with heterotrophic granules. Appl Microbiol Biotechnol 100(21):9381–9391. https://doi.org/10.1007/s00253-016-7797-9

Wang L, Zheng P, Chen TT, Chen JW, Xing YJ, Ji QX, Zhang M, Zhang J (2012) Performance of autotrophic nitrogen removal in the granular sludge bed reactor. Bioresour Technol 123:78–85. https://doi.org/10.1016/j.biortech.2012.07.112

Wang L, Zheng P, Xing YJ, Li W, Yang J, Abbas G, Liu S, He ZF, Zhang JQ, Zhang HT, Lu HF (2014) Effect of particle size on the performance of autotrophic nitrogen removal in the granular sludge bed reactor and microbiological mechanisms. Bioresour Technol 157:240–246. https://doi.org/10.1016/j.biortech.2014.01.116

Wang S, Liu Y, Niu Q, Ji J, Hojo T, Li YY (2017) Nitrogen removal performance and loading capacity of a novel single-stage nitritation-anammox system with syntrophic micro-granules. Bioresour Technol 236:119–128. https://doi.org/10.1016/j.biortech.2017.03.164

Zhang BG, Liu Y, Tong S, Zheng MS, Zhao YX, Tian CX, Liu HY, Feng CP (2014a) Enhancement of bacterial denitrification for nitrate removal in groundwater with electrical stimulation from microbial fuel cells. J Power Sources 268:423–429. https://doi.org/10.1016/j.jpowsour.2014.06.076

Zhang JB, Zhou J, Han Y, Zhang XG (2014b) Start-up and bacterial communities of single-stage nitrogen removal using anammox and partial nitritation (SNAP) for treatment of high strength ammonia wastewater. Bioresour Technol 169:652–657. https://doi.org/10.1016/j.biortech.2014.07.042

Zhang XJ, Zhang HZ, Ye CM, Wei MB, Du JJ (2015) Effect of COD/N ratio on nitrogen removal and microbial communities of CANON process in membrane bioreactors. Bioresour Technol 189:302–308. https://doi.org/10.1016/j.biortech.2015.04.006

Zheng BY, Zhang L, Guo JH, Zhang SJ, Yang AM, Peng YZ (2016) Suspended sludge and biofilm shaped different anammox communities in two pilot-scale one-stage anammox reactors. Bioresour Technol 211:273–279. https://doi.org/10.1016/j.biortech.2016.03.049